UDK 669.24

Sibirskii Gosudarstvennyi Aerokosmicheskii Universitet
imeni Akademika M. F. Reshetneva. Vestnik
Vol. 18, No. 1, P. 211–218

MAGNETIC PROPERTIES OF PLASTICALLY DEFORMED NICKEL-TITANIUM ALLOY

F. M. Noskov[1], A. V. Nyavro[2], V. N. Cherepanov[2], A. K. Drozdova[2], L. I. Kveglis[1]

[1]Siberian Federal University
79/10, Svobodnyy Av., Krasnoyarsk, 660041, Russian Federation
[2]National Research Tomsk State University
36, Lenina Av., Tomsk, 634050, Russian Federation
E-mail: kveglis@list.ru

Ni–Ti alloy has been intensively studied over the past decades. The unique properties of the alloy have allowed using it as a structural material for the creation of instruments and devices in various fields of science and technology, including mechanical engineering, aerospace, instrumentation. Measuring magnetic hysteresis loop is shown that after the deformation of the alloy having ferromagnetic properties. According to the equilibrium phase diagram, the alloys of Ni–Ti at a Ti content above 10 at. % is non-ferromagnetic. Due to lowering of the crystal phase symmetry with a cubic lattice the magnetization appears. In this work we have investigated the magnetic properties and the structure of deformed $Ni_{51}Ti_{49}$ samples by electron microscopy and X-ray diffraction methods. In $Ni_{51}Ti_{49}$ samples after plastic deformation the lenticular crystals containing bending contours with a high concentration of internal stresses were found. Bending contours indicate a large distortion of the crystal lattice. The curvature of the crystal lattice occurs due to the large displacements of the atoms. As a result, it can be formed and icosahedral cluster with the structure of the Frank–Kasper. An icosahedron is a twelve vertex polyhedron, which is denoted by FK-12. Furthermore, the crystal can be formed in other Frank–Kasper structures, e. g., FK-16. FK-16 is a sixteen vertex polyhedron with atom located in the center of the cluster. Indexing paintings electron diffraction and X-ray showed that the alloy phase of the Ni–Ti coexist with the structure Ti_2Ni and Ni_4Ti_3. For explaining the possibility of the appearance of magnetization in Ni–Ti alloy samples spin-polarized electron density of states and magnetic moments $Ni_{10}Ti_6$ clusters (FK-16), Ni_7Ti_5 (FK-12) alloy $Ni_{51}Ti_{49}$ for electrons with different spin projections: "up" and "down" was calculated. The calculation by the scattered waves (RF) was performed. The results of calculation can be seen that the total electron density of nickel tends to zero faster than the density of titanium. Also shows that nickel becomes negative spin density in the area of r = 3.25–6.7 a. u. and titanium for r > 4.5 a. u. This may result depending on the value of the interatomic distances and to the effects ferromagnetism and antiferromagnetic in order to establish a magnetic clusters. The spectra show a high density of states near the Fermi level that is a characteristic feature of metals, besides there is an increase in the magnetization of the alloy during deformation. The calculations showed that the investigated clusters, not susceptible to deformation, also have a magnetic moment (the average magnetic moment per atom cluster FK-12, is about 1,0 μ_B, and for the FK-16 is about 0.3 μ_B. Overall, however, the average magnetic moment is zero, due to the absence of a preferred direction (the chaotic distribution of clusters) for the alloy. However, if the cluster is subjected to tension, the compensation of the magnetic moments of clusters occurs in the alloy, since there is allocated for all atoms direction due to deformation. At the same time, the average magnetic moments of the atoms in the cluster for the Deformed increase to 1.6 μ_B and 0.8 μ_B respectively for the FK-12 and FK-16.

Keywords: titanium nickel alloy, ferromagnetic properties, lenticular crystal cluster, the icosahedron, pentagonal symmetry, spin-polarized electron density of states.

Вестник СибГАУ
Том 18, № 1. С. 211–218

МАГНИТНЫЕ СВОЙСТВА В ПЛАСТИЧЕСКИ ДЕФОРМИРОВАННОМ НИКЕЛЬ-ТИТАНОВОМ СПЛАВЕ

Ф. М. Носков[1], А. В. Нявро[2], В. Н. Черепанов[2], А. К. Дроздова[2], Л. И. Квеглис[1]

[1]Сибирский федеральный университет
Российская Федерация, 660041, г. Красноярск, просп. Свободный, 79/10
[2]Национальный исследовательский Томский государственный университет
Российская Федерация, 634050, г. Томск, просп. Ленина, 36
E-mail: kveglis@list.ru

Сплавы системы Ni–Ti интенсивно изучаются в течение последних десятилетий. Уникальные свойства сплава позволили использовать его в качестве конструкционного материала для создания приборов и устройств в различных областях науки и техники, в том числе машиностроении, аэрокосмической сфере, приборостроении. Показано, что после деформации сплав $Ni_{51}Ti_{49}$ приобретает ферромагнитные свойства. Согласно равновесной фазовой диаграмме, сплавы Ni–Ti при содержании Ti выше 10 ат. % не являются ферромагнитными. Известно, что за счет понижения симметрии кристаллической фазы с кубической решеткой возможно возникновение намагниченности. Исследованы магнитные свойства и структура деформированных образцов $Ni_{51}Ti_{49}$ с помощью методов электронной микроскопии и дифракции рентгеновских лучей. В образцах $Ni_{51}Ti_{49}$ после пластической деформации найдены линзовидные кристаллы, содержащие изгибные контуры с высокой концентрацией внутренних напряжений. Изгибные экстинкционные контуры указывают на искажение кристаллической решетки, поскольку кривизна кристаллической решетки возникает при больших смещениях атомов. В результате таких смещений в сплаве могут быть сформированы икосаэдрические кластеры со структурой Франка–Каспера. Икосаэдр – это двенадцативершинник, который обозначается как ФК-12. Кроме того, кристалл может быть сформирован в других структурах Франка–Каспера, например ФК-16, который представляет собой шестнадцативершинник с атомом, расположенным в центре кластера. Расшифровка картины дифракции электронов и рентгеновских лучей показала, что в сплаве Ni–Ti могут сосуществовать фазы Ti_2Ni и Ni_4Ti_3. Для объяснения возможности появления намагниченности в образцах сплава Ni–Ti делался расчет плотности спин-поляризованных состояний электронов для кластеров $Ni_{10}Ti_6$ (ФК-16) и Ni_7Ti_5 (ФК-12) сплава $Ni_{51}Ti_{49}$. Расчет выполнялся методом рассеянных волн. Показано, что полная плотность электронов никеля быстрее стремится к нулю, чем плотность титана. Показано, что спиновая плотность никеля становится отрицательной на расстоянии порядка $r = 3{,}25–6{,}7$ а. е., а титана – при $r > 4{,}5$ а. е. Такие значения r соответствуют межатомным расстояниям в кластерах, которые могут сильно изменяться при деформации. Как следствие, это может приводить к эффектам как ферромагнитизма, так и антиферромагнитизма при установлении магнитного порядка в кластерах, в зависимости от величины межатомных расстояний. Расчетные спектры показывают высокую плотность состояний вблизи уровня Ферми, что является характерной особенностью ферромагнитных металлов. Расчеты показали, что исследуемые кластеры восприимчивы к деформации, а также обладают магнитным моментом (у неискаженного кластера средний магнитный момент на атом кластера ФК-12 составляет около 1,0 μ_B, а для ФК-16 он составляет около 0,3 μ_B). Однако общий средний магнитный момент равен нулю из-за отсутствия предпочтительного направления (хаотическое распределение кластеров) для сплава. В случае же, когда атомы кластера смещены (искаженный кластер), спины атомов (↑ и ↓) не компенсируют друг друга, вследствие чего у искаженного кластера появляется магнитный момент больший, чем у неискаженного кластера, соответственно 1,6 и 0,8 μ_B на один атом для ФК-12 и ФК-16.

Ключевые слова: сплавы Ni–Ti, ферромагнитные свойства, кластеры в линзовидных кристаллах, икосаэдр, пентагональная симметрия, плотности спин-поляризованных электронных состояний.

Introduction. Ni–Ti alloy has been intensively studied over the past decades. Shape memory effect found in this alloy [1] has attracted the attention of many researchers. The unique properties of the alloy have allowed using it as a structural material for the creation of instruments and devices in various fields of science and technology, including mechanical engineering, aerospace, instrumentation. Especially it is important the use of this alloy in medicine [2; 3]. Due to the accumulation of new knowledge the scope of this material is continually expanding.

In our previous article [4] the structure of the bulk $Ni_{51}Ti_{49}$ alloy specimens under tensile loading was studied. Electron microscopy and electron diffraction methods are applied to show that a phase with FCC lattice can be present in titanium nickelide. We have shown that interplanarspacings BCC_{110}, FCC_{111} and HCP_{002} for the studied alloy have close values which demonstrate the possibility of their mutual polymorphic transformation.

We previously investigated the magnetic states of deformed samples by torsion magnetometer method after various numbers of cyclic martensite transformations. Torsion curves have shown the magnetization appearance in $Ni_{51}Ti_{49}$ samples after various numbers of direct and reverse transformations [5]. The phase with a non-zero volume magnetization was formed in the samples during the cyclic martensite transformations. The ferromagnetic phase is distributed in the sample heterogeneously.

We suggested that processes occurringof ferromagnetic properties are the result of repeated direct-reverse martensite transition cycles in Ni–Ti alloys and can lead to the isolation of ferromagnetic particles that are rich in nickel [5; 6]. According to the equilibrium phase diagram, the alloys of Ni–Ti at a Ti content above 10 at. % is non-ferromagnetic. Another hypothesis for appearance of ferromagnetic properties in $Ni_{51}Ti_{49}$ alloy after plastic deformation concerns with the appearance of intermetallide phases [7]. Moreover, by lowering the symmetry of the crystal phase with a cubic lattice the magnetization of alloy appears [8; 9].

Experimental results and discussion. In this work we have investigated the magnetic properties and the structure of deformed $Ni_{51}Ti_{49}$ samples by electron microscopy and X-ray diffraction methods. In fig. 1 we can see the different types of hysteresis loop before and after plastic deformation [10].

The numerous of martensite transformation features in Ni–Ti alloys (e. g. transformation temperature, presence and amount of intermediate phases, nature and mechanism of martensitetransformation) is highly dependent on the availability of lenticular nanocrystals of Ni_4Ti_3 phase. The researches [11] showed the appearance

of lenticular single crystals by exposure to electron beam in metal amorphous films and metal compounds. In $Ni_{51}Ti_{49}$ samples after plastic deformation the lenticular crystals containing bending contours with a high concentration of internal stresses were found. TEM imageofthis crystals is shown in fig. 2.

Lenticular crystals contain a large amount of bending contours. Bending contours indicate a large distortion of the crystal lattice. The curvature of the crystal lattice occurs due to the large displacements of the atoms. The result is the transformation of the original BCC (body-centered cubic) lattice in the FCC (face-centered cubic) lattice, as shown in [4]. FCC lattice contains clusters: tetrahedra and octahedra. Shift and rotation of octahedrons and tetrahedrons results in the formation of the hexagonal lattice. According to [12] octahedra can be transformed into tetrahedrons. As a result, it can be formed and icosahedral cluster with the structure of the Frank-Kasper. An icosahedron is a twelve vertex polyhedron, which is denoted by FK-12. Furthermore, the crystal can be formed in other Frank–Kasper structures, e. g., FK-16. FK-16 is a sixteen vertex polyhedron with atom located in the center of the cluster. This structure is shown in work [13].

Indexing paintings electron diffraction and X-ray showed that the alloy phase of the Ni–Ti coexist with the structure Ti_2Ni and Ni_4Ti_3. X-ray diffraction of the sample of alloy$Ni_{51}Ti_{49}$ is shown in fig. 3. Both phases have a spinel structure and may be coherently linked: Ti_2Ni + Ni_4Ti_3 = 5NiTi. The possibility of coexistence of these phases, as partners, was shown by Kraposhin [12; 14].

For explaining the possibility of the appearance of magnetization in Ni–Ti alloy samples spin-polarized electron density of states and magnetic moments $Ni_{10}Ti_6$ clusters (FK-16), Ni_7Ti_5 (FK-12) alloy $Ni_{51}Ti_{49}$ for electrons with different spin projections: “up” and “down” was calculated. The calculation by the scattered waves (RF) was performed [15]. To build a “muffin-tin” building electron densities for $Ni_{10}Ti_6$ clusters and the one-electron energy levels of nickel and titanium atoms based on the unrestricted Hartree-Fock (UHF) with the exchange-correlation potential Gunnarsson – Lundqvist was calculated [16]. This potential can effectively describe the magnetic states as atoms, and the entire cluster as a whole [17]. In this case UHF method system of equations can be written as:

$$\left[-\frac{d^2}{dr^2}+\frac{l(l+1)}{r^2}-\frac{2Z}{r}+V_C(r)-V_{XGL}^{\sigma}(r)\right]P_{nl\sigma}(r)= \\ =\varepsilon_{nl\sigma}P_{nl\sigma}(r). \quad (1)$$

The number of equations in the system (1) is the number accounted for subshells of the atom considered, ie the number of sets of quantum states carried with numbers $\{nl\sigma\}$. Further, the system of equations (1): Z – nuclear charge; $P_{nl\sigma}$ (r) – the radial wave function describing the state of electrons in a subshell on the quantum numbers $\{nl\sigma\}$, where σ determines the spin projection on the z-axis; V_C (r) – the potential of the Coulomb interaction of the electrons; the exchange interaction potential Gunnarsson–Lundqvist [18].

Solving the system of equations (1) and nickel titanium atoms shells electron levels received energy and the wave functions of those atoms as a function of the spin components. The computed one-electron energy levels are shown in table. From table it follows that external electronic shells of atoms cleaved stronger than internal, which have almost no splitting.

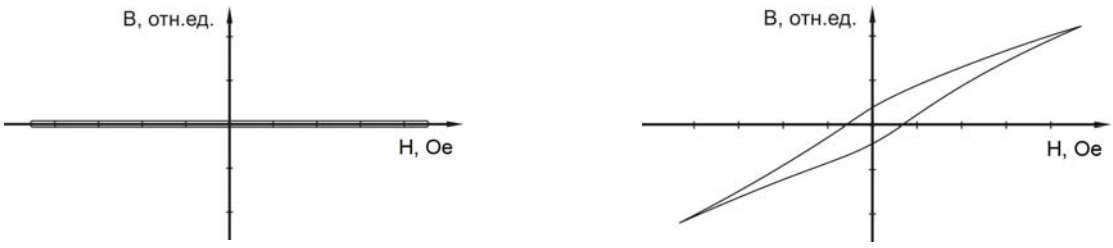

a *b*

Fig. 1. Types of hysteresis loop before (*a*) and after (*b*) plastic deformation (scale on the horizontal axis corresponds to H = 250 Oe [10])

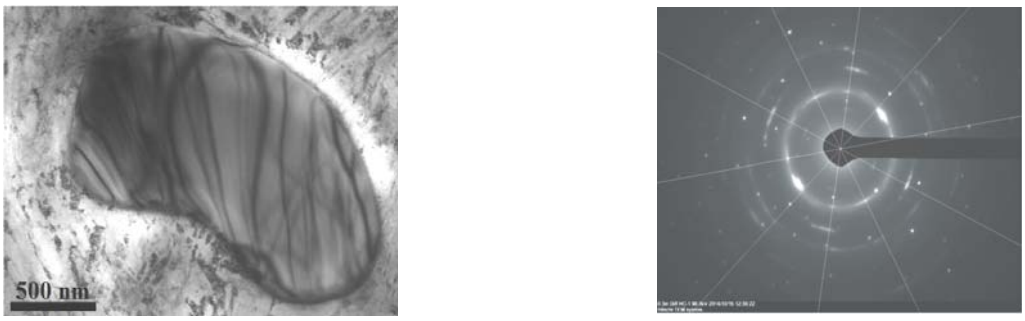

a *b*

Fig. 2. TEM image of the area of origin of lenticular crystals containing bending contours with a high concentration of internal stresses were found in $Ni_{51}Ti_{49}$ samples after plastic deformation (*a*); electron diffraction pattern of the site with pentagonal symmetry (*b*)

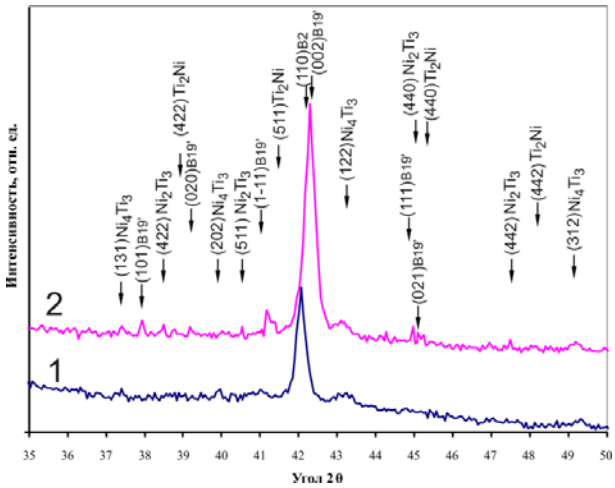

Fig. 3. X-ray diffraction of the sample of alloy $Ni_{51}Ti_{49}$:
1 – $M = 0$; 2 – $M > 0$ (M is saturation magnetization)

One-electron energy levels of the titanium and nickel atoms

Ti		Ni	
$nl\sigma$	$\lvert E_{nl}\rvert$, Ry	$nl\sigma$	$\lvert E_{nl}\rvert$, Ry
$1s^{1\uparrow}$	354.51197	$1s^{1\uparrow}$	595.74822
$1s^{1\downarrow}$	354.51291	$1s^{1\downarrow}$	595.74708
$2s^{1\uparrow}$	38.91297	$2s^{1\uparrow}$	70.67054
$2s^{1\downarrow}$	38.86277	$2s^{1\downarrow}$	70.56912
$2p^{3\uparrow}$	32.56451	$2p^{3\uparrow}$	61.77916
$2p^{3\downarrow}$	32.52616	$2p^{3\downarrow}$	61.70268
$3s^{1\uparrow}$	4.53472	$3s^{1\uparrow}$	7.93867
$3s^{1\downarrow}$	4.36985	$3s^{1\downarrow}$	7.73841
$3p^{3\uparrow}$	2.86531	$3p^{3\uparrow}$	5.22452
$3p^{3\downarrow}$	2.69807	$3p^{3\downarrow}$	5.02787
$3d^{2\uparrow}$	0.36168	$3d^{5\uparrow}$	0.72999
$4s^{1\uparrow}$	0.28178	$3d^{3\downarrow}$	0.55371
$4s^{1\downarrow}$	0.35532	$4s^{1\uparrow}$	0.43240
		$4s^{1\downarrow}$	0.39915

The wave functions obtained by solving the equation (1), were used for calculation of total electron densities and spin basic configuration of titanium and nickel atoms. In accordance with rule of Gund, in the ground state of an atom of titanium in the unfilled 3d shell is just 2 electrons with parallel spins ($3d^2$ configuration), and the nickel atom, on the contrary, to fill the 3d shell lacks 2 electrons. 3d electron configuration for nickel has the following form: $3d^5 3d^3$. The presence of unfilled d-shell electrons of the atoms leads to the effect of "spin polarization", that's the energy levels of all the shells are broken down according to the projection of the spin. In the calculation we used the following configuration of the ground states of the atoms:

$$\begin{aligned}&\text{Ti: } 1s^{1\uparrow}1s^{1\downarrow}2s^{1\uparrow}2s^{1\downarrow}2p^{3\uparrow}2p^{3\downarrow}\\&3s^{1\uparrow}3s^{1\downarrow}3p^{3\uparrow}3p^{3\downarrow}3d^{2\uparrow}4s^{1\uparrow}4s^{1\downarrow},\\&\text{Ni: } 1s^{1\uparrow}1s^{1\downarrow}2s^{1\uparrow}2s^{1\downarrow}2p^{3\uparrow}2p^{3\downarrow}3s^{1\uparrow}\\&3s^{1\downarrow}3p^{3\uparrow}3p^{3\downarrow}3d^{5\uparrow}3d^{3\downarrow}4s^{1\uparrow}4s^{1\downarrow}.\end{aligned} \quad (2)$$

Full density of electrons in the atom can be represented as:

$$\rho(r) = \frac{1}{4\pi}\sum_{i\sigma} n_{i\sigma}\left|R_{i\sigma}(r)\right|^2, \quad (3)$$

where $n_{i\sigma}$ – the number of fill subshells with different spin projections, radial functions $R_{i\sigma}(r) = \frac{R_{nl\sigma}(r)}{r}$.

The spin density of the electrons is determined by the difference in the electron density of atoms with spin "up" and "down":

$$\rho(r) = \rho^{\uparrow}(r) + \rho^{\downarrow}(r). \quad (4)$$

The results of calculation of the total spin and electron densities of Ni and Ti atoms are shown in fig. 4. It can be seen that the total electron density of nickel tends to zero faster than the density of titanium. This is due to the fact that the charge of nickel anymore, he strongly attracts electrons to the nucleus than titanium. Fig. 4, *b* also shows that nickel becomes negative spin density in the area of r = 3.25–6.7 a. u. and titanium for $r > 4.5$ a. u. This may result depending on the value of the interatomic distances and to the effects ferromagnetism and anti-ferromagnetic in order to establish a magnetic clusters. In addition, most titanium delocalization spin density (in both its positive and in the negative areas) contributes to the fact that the magnetic moment of the titanium atom in the compounds is not manifested.

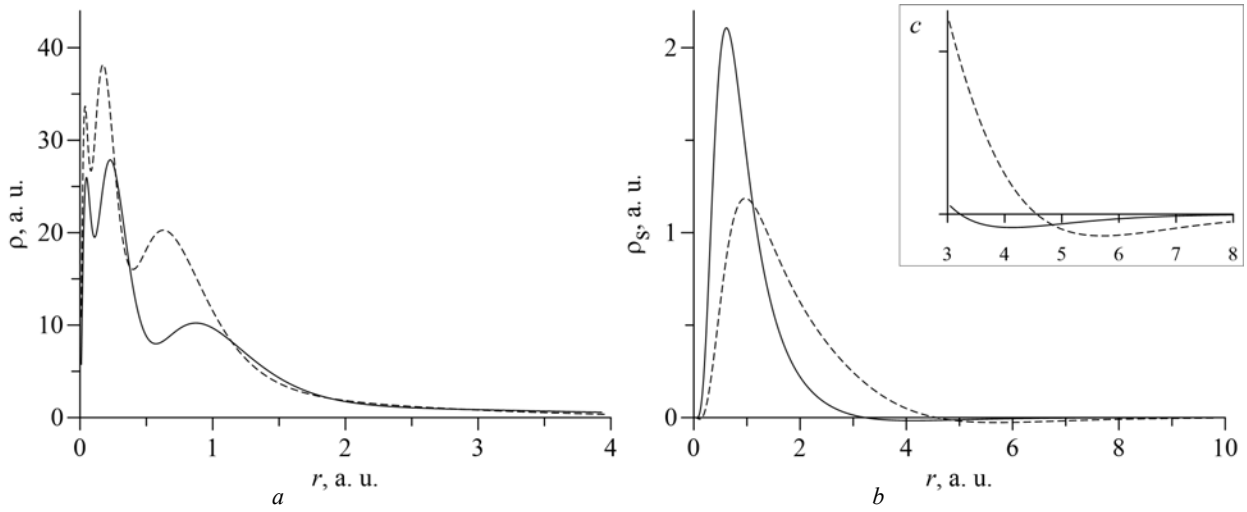

Fig. 4. Total (*a*) and spin (*b*) electron density for titanium and nickel atoms:
solid line – for Ni atoms; dashed line – for the Ti atoms; *c* – enlarged fragment

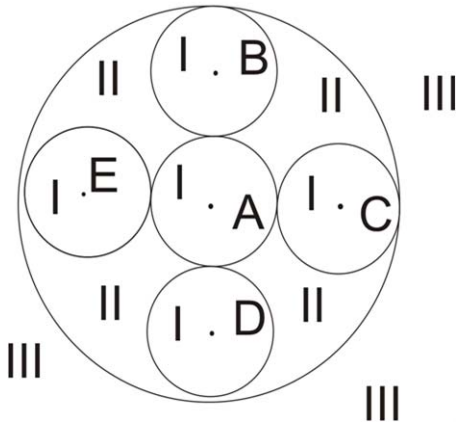

Fig. 5. Splitting the potential cluster into three regions by the method of scattered waves:
I – the area of atomic spheres; II – Intersectoral space; III – the scope Watson

The calculated electron density (3) and (4) continue to be used for the construction of "muffin-tin" potential clusters of FC-16 and FC-12 on the basis of PB method. The potential of the cluster is divided into three regions: the atomic spheres (I), intersectoral space (II) and the scope of Watson (III) (fig. 5).

Using a "muffin-tin" approximation [19] for the cluster-building makes it relatively easy to find a solution to the one-electron equation for each of the regions of the molecule or cluster. The approximation of a spherical symmetry allows to separate the variables in the Schrodinger equation, and the wave function of each of the one-electron states represented as the product of radial and angular parts. Using the condition of "stitching" of the wave function at the border areas of section (I)–(III), can be prepared secular equation for calculation of the spectrum of a molecule or cluster as [17; 19]:

$$\det\left\|\left[t_l^p\right]^{-1}\delta_{ll'}\delta_{mm'}-\sum_{\substack{q\neq p\\ l'm}}G_{lm,l'm'}^{pq}\left(\varepsilon_i\right)\right\|=0. \qquad (5)$$

In equation (5) used the notation of [17]. Determinants'zeros (5) give the values of the energy levels of the cluster. It should be noted that the effectiveness of the approach used to study the properties of the Frank–Kasper structures illustrated by the example of iron and manganese alloys in [20].

Calculated using the formula (5) one-electron energy levels of the clusters were used to calculate the electron density of states $N(E)$. For this purpose, limited to consideration of the electronic structure of small clusters, you must take into account the discrete electron levels (the number of one-electron levels still not large enough to form a continuous distribution of electronic states). To compare the calculation results with the experimental data, as well as with the results of calculations using the methods of band theory, each discrete energy level is comparable to the distribution function of the energy density in the form of a Gaussian:

$$n_i\left(E\right)=\frac{n_i}{\gamma\sqrt{2\pi}}\exp\left[-\frac{\left(E-\varepsilon_i\right)^2}{2\gamma^2}\right], \qquad (6)$$

where n_i – occupation number of the *i*-th level, and setting determines the degree of blurring of the energy state (γ = 0.015Ry). Using a distribution $n_i(E)$ in the form (6) makes it possible to limit the transition from cluster to an infinite crystal. Then the total density of electronic states in the cluster is given by:

$$N(E) = \sum_i n_i(E). \quad (7)$$

The magnetic moment of the *p*-th atom in the cluster is determined in accordance with [19], the following expression:

$$\mu_p = \int_{-\infty}^{E_F} N_p^{\uparrow}(E)dE - \int_{-\infty}^{E_F} N_p^{\downarrow}(E)dE. \quad (8)$$

Here $N_p^{\uparrow(\downarrow)}(E) = \sum_l N_{pl}^{\uparrow(\downarrow)}(E)$ – is local spin density of electrons *p*-th atom, defined by the formula (6) and (7) for each atom with spin. Fig. 5 and 6 shows the results of calculations of the spin density of electronic states $N^{\uparrow(\downarrow)}(E) = \sum_p N_p^{\uparrow(\downarrow)}(E)$ for Ni_7Ti_5 clusters and $Ni_{10}Ti_6$ $Ni_{51}Ti_{49}$ alloy for undeformed (near-spherical structure), and for the cluster of deformed (elongated by 5 % along the Z-axis), respectively. Unfortunately, the authors of [21] did not give any information about the magnetization of the alloy.

The spectra in fig. 6 and 7 show a high density of states near the Fermi level that is a characteristic feature of metals, besides there is an increase in the magnetization of the alloy during deformation.The calculations showed that the investigated clusters, not susceptible to deformation, also have a magnetic moment (the average magnetic moment per atom cluster FK-12, is about 1.0 μ_B, and for the FK-16 is about 0.3 μ_B. Overall, however, the average magnetic moment is zero, due to the absence of a preferred direction (the chaotic distribution of clusters) for the alloy. However, if the cluster is subjected to tension, the compensation of the magnetic moments of clusters occurs in the alloy, since there is allocated for all atoms direction due to deformation. At the same time, the average magnetic moments of the atoms in the cluster for the Deformed increase to 1.6 μ_B and 0.8 μ_B respectively for the FK-12 and FK-16.

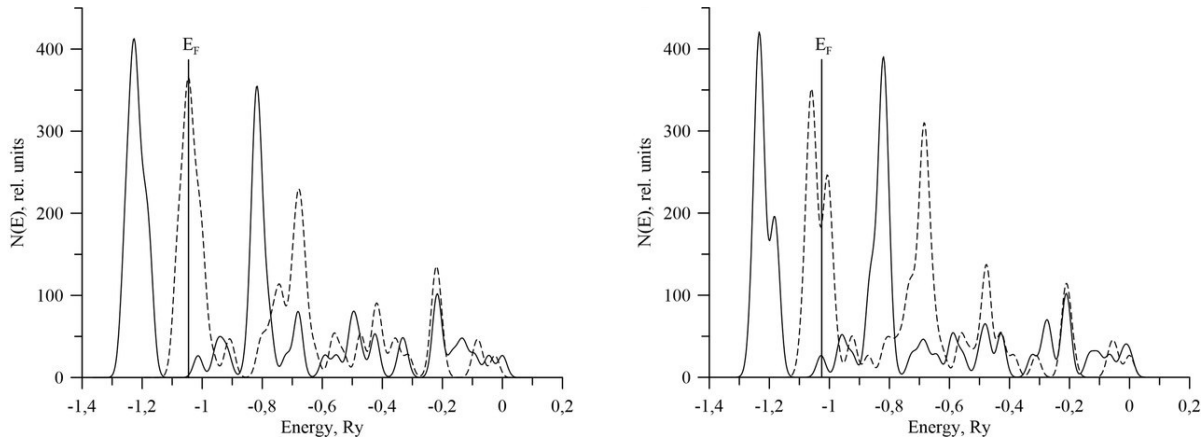

Fig. 6. The distribution of the electron density of states $N(E)$ for Ni_7Ti_5 clusters: deformed cluster (*a*); non-deformed cluster (*b*). Solid line corresponds to the density of electrons with spin "up" (↑), dashed line – with spin "down" (↓); E_F – the position of the Fermi level

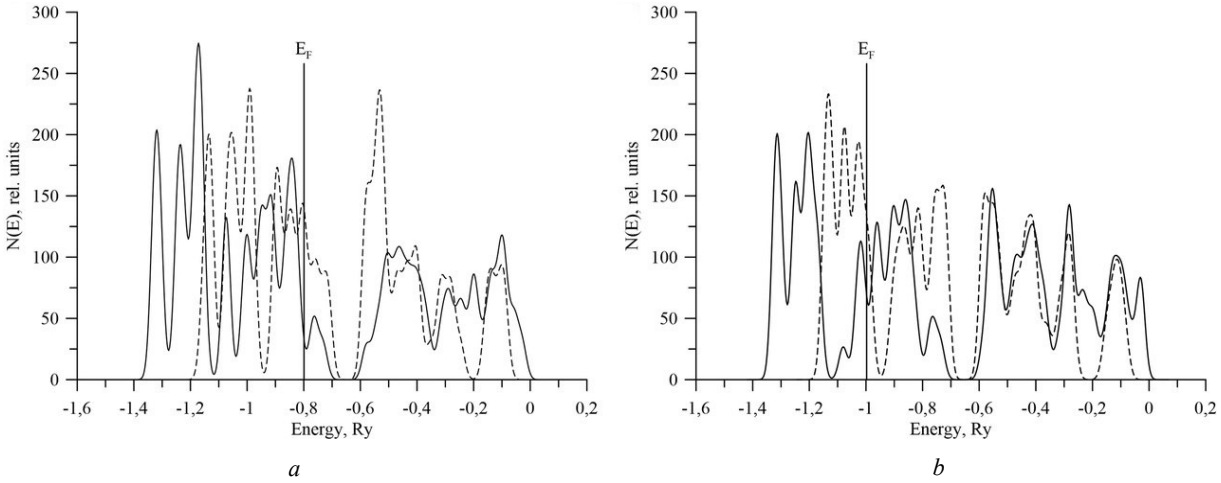

Fig. 7. The distribution of the electron density of states $N(E)$ for $Ni_{10}Ti_6$ clusters: deformed cluster (*a*); non-deformed cluster (*b*). Solid line corresponds to the density of electrons with spin "up" (↑), dashed line – with spin "down" (↓); E_F – the position of the Fermi level

Conclusions. Experimental and theoretical study of $Ni_{51}Ti_{49}$ alloy showed the appearance of magnetization in its deformation (stretching), connected with the lowering of crystal symmetry with B2 structure. It is also shown the possibility of existence of phase with FCC for NiTi. It was found that the interplanar distance BCC110, FCC111 and HCP002 in these alloys have similar values, indicating the possibility of their mutual polymorphic transformation. The new scheme of martensitic transformations in NiTi of B2 structure (BCC) in B19′ (HCP lattice) through the intermediate phase of FCC.

Acknowledgments. The authors are grateful to the staff of the Laboratory IRGETAS East Kazakhstan State Technical University, A. Dzhes for help with the experiment.

Благодарности. Авторы благодарят сотрудника лаборатории ИРГЕТАС Восточно-Казахстанского государственного технического университета А. В. Джес за помощь в проведении эксперимента.

References

1. Gunter V. E., Yasenchuk Y. F., Klopotov A. A., Khodorenko V. N. [Physical and mechanical properties and structure of the porous alloy superelastic TiNi]. *Pis'ma v ZhTF*. 2000, Vol. 26, No. 1, P. 71–76 (In Russ.).

2. Gunter V. E., Dombaev G. T., Sysolyatin P. G. et al. *Meditsinskie materialy i implantaty s pamyat'yu formy* [Medical Materials and Implants with Shape Memory]. Tomsk, TGU Publ., 1998, 486 p.

3. Itin V. I., Shevchenko N. A., Korostelyova E. N., Tuhfatullin A. A., Mirgazizov M. Z., Gunter V. E. [Functional composites "bioceramics titanium-nickel alloy" for medicine]. *Pis'ma v ZhTF*. 1997, Vol. 23, No 8, P. 1–6 (In Russ.).

4. Kveglis L. I., Noskov F. M., Volochaev M. N., Jess A. V. [Martensitic transformations in NiTi through an intermediate phase with FCC]. *Fizicheskaja mezomehanika*. 2016, Vol. 19, No. 2, P. 100–107 (In Russ.).

5. Abylkalykova R. B., Tazhibaeva G. B., Noskov F. M., Kveglis L. I. Features of martensitic transformation in NiTi. *Bulletin of the Russian Academy of Sciences: Physics*. 2009, Vol. 73, No. 11, P. 1542–1544.

6. Panin V. E., Egorushkin V. E. [Curvature Solitons as Generalized Structural Wave Carriers of Plastic Deformation and Fracture]. *Fizicheskaya mezomekhanika*. 2013, Vol. 16, No. 4, P. 267–286 (In Russ.).

7. Takacs L. Mechanochemistry and the Other Branches of Chemistry: Similarities and Dierences. *Acta physica polonica A*. 2012, Vol. 121, No. 3, P. 711–714.

8. Khomskii D. I., Kugel K. I., Sboychakov A. O., Streltsov S. V. Role of local geometry in the spin and orbital structure of transition metal compounds. *JETP letters*. 2016, Vol. 122, No 3, P. 484.

9. Gudenough J. B. Magnetism and the Chemical Bond. New York, Wiley Intersci. 1963, 394 p.

10. Frolov G. I., Zhigalov V. S. *Fizicheskie svoystva i primenenie magnitoplenochnykh nanokompozitov* [Physical properties and application of nanocomposite magnetic films]. Novosibirsk, SB RAS Publ., 2006, 187 p.

11. Kolosov V. Yu., Tholen A. R. Transmission electron microscopy studies of the specific structure of crystals formed by phase transition in iron oxide amorphous films. *Acta Materialia*. 2000, Vol. 48, P. 1829.

12. Talis A., Kraposhin V. Finite noncrystallographic groups, 11-vertex equi-edged triangulated clusters and polymorphic transformations in metals. *ActaCryst.* 2014, Vol. A70, P. 616–625.

13. Kveglis L. I., Dzhes A. V., Volochaev M. N., Cherkov A. G., Noskov F. M. The clusters self-assembled crystal and magnetic structure during the martensite transition in $Fe_{86}Mn_{13}C$ alloy. *Journal of Siberian Federal University. Engineering & Technologies.* 2015, Vol. 8, No. 1, P. 48–56.

14. Kraposhin V. S., Talis A. L., Demin E. D., Zaitsev A. I. [Crystal geometry and mechanism of fusion of spinel manganese sulfide in complex non-metallic inclusion]. *Metallovedenie i termicheskaya obrabotka metallov*. 2015, Vol. 7, P. 4–12 (In Russ.).

15. Slater J. C., Johnson K. H. Self-consistent field X_α cluster method for polyatomic molecules and solids. *Phys. Rev. B*. 1972, Vol. 5, No. 3, P. 844–853.

16. Slater J. C. Suggestions from solid-state theory regarding molecular calculations. *J. Chem. Phys.* 1985, Vol. 43, P. 228.

17. Nyavro A. V. *Evolyutsiya elektronnykh sostoyaniy: atom – molekula – klaster – kristall* [Evolution of electronic states: atom-molecule-cluster-crystal]. Tomsk, TGU Publ., 2013, 268 p.

18. Gunnarson O., Lundqvist B. I. Exchange and correlation in atoms, molecules and solids by the spin-density-functional formalism. *Phys. Rev. B*. 1976, Vol. 13, No. 10, P. 4274–4298.

19. Nemoshkalenko V., Kucherenko N. *Metody vychislitel'noy fiziki v teorii tverdogo tela. Elektronnye sostoyaniya v neideal'nykh kristallakh* [Methods of computational physics in solid state theory. Electronic states in imperfect crystals]. Kiev, Naukova Dumka Publ., 1986, 296 p.

20. Kveglis L. I., Abylkalykova R. B., Noskov F. M., Arhipkin V. G., Musikhin V. A., Cherepanov V. N., Niavro A. V. Local electron structure and magnetization in β – $Fe_{86}Mn_{13}C$. *Superlattices and Microstructures.* 2009, Vol. 46, No. 1–2, P. 114–120.

21. Kulkova S. E., Valuysky D. V., Smolin I. Y. [Changes in the electronic structure at B2-B19' martensitic transformation in NiTi]. *Fizika tverdogo tela*. 2001, Vol. 43, No. 4, P. 706–713 (In Russ.).

Библиографические ссылки

1. Физико-механические свойства и структура сверхэластичных пористых сплавов на основе никелида титана / В. Э. Гюнтер [и др.] // Письма в ЖТФ. 2000. Т. 26, № 1. С. 71–76.

2. Медицинские материалы и имплантаты с памятью формы / В. Э. Гюнтер [и др.]. Томск : ТГУ, 1998. 486 с.

3. Функциональные композиционные материалы «биокерамика – никелид титана» для медицины / В. И. Итин [и др.] // Письма в ЖТФ. 1997. Т. 23, № 8. С. 1–6.

4. Мартенситные превращения в никелиде титана через промежуточную фазу с ГЦК-решеткой / Л. И. Квеглис [и др.] // Физическая мезомеханика. 2016. Т. 19, № 2. С. 100–107.

5. Особенности мартенситного превращения в никелиде титана / Р. Б. Абылкалыкова [и др.] // Известия Российской академии наук. Серия физическая. 2009. Т. 73, № 11. С. 1642–1644.

6. Панин В. Е., Егорушкин В. Е. Солитоны кривизны как обобщенные волновые структурные носители пластической деформации и разрушения // Физическая мезомеханика. 2013. Т. 16, № 3. С. 7–26.

7. Takacs L. Mechanochemistry and the Other Branches of Chemistry: Similarities and Dierences // Acta physica polonica A. 2012. Vol. 121, No 3. P. 711–714.

8. Role of local geometry in the spin and orbital structure of transition metal compounds / D. I. Khomskii [et al.] // JETP letters. 2016. Vol. 122, No 3. P. 484.

9. Gudenough J. B. Magnetism and the Chemical Bond. New York : Wiley Intersci., 1963. 394 p.

10. Фролов Г. И., Жигалов В. С. Физические свойства и применение магнитопленочных нанокомпозитов. Новосибирск : Изд-во СО РАН, 2006. 187 с.

11. Kolosov V. Yu., Tholen A. R. Transmission electron microscopy studies of the specific structure of crystals formed by phase transition in iron oxide amorphous films // Acta Materialia. 2000. Vol. 48. P. 1829.

12. Talis A., Kraposhin V. Finite noncrystallographic groups, 11-vertex equi-edged triangulated clusters and polymorphic transformations in metals // ActaCryst. 2014. Vol. A70. P. 616–625.

13. The clusters self-assembled crystal and magnetic structure during the martensite transition in $Fe_{86}Mn_{13}C$ alloy / L. I. Kveglis [et al.] // Journal of Siberian Federal University. Engineering & Technologies. 2015. Vol. 8, No 1. P. 48–56.

14. Кристаллогеометрический механизм срастания шпинели и сульфида марганца в комплексное неметаллическое включение / В. С. Крапошин [и др.] // Металловедение и термическая обработка металлов. 2015. № 7. С. 4–12.

15. Slater J. C., Johnson K. H. Self-consistent field Xα cluster method for polyatomic molecules and solids // Phys. Rev. B. 1972. Vol. 5, No 3. P. 844–853.

16. Slater J. C. Suggestions from solid-state theory regarding molecular calculations // J. Chem. Phys. 1985. Vol. 43. P. 228.

17. Нявро А. В. Эволюция электронных состояний: атом–молекула–кластер–кристалл. Томск : Томский гос. ун-т, 2013. 267 с.

18. Gunnarson O., Lundqvist B. I. Exchange and correlation in atoms, molecules and solids by the spin-density-functional formalism // Phys. Rev. B. 1976. Vol. 13, No 10. P. 4274–4298.

19. Немошкаленко В. В., Кучеренко Ю. Н. Методы вычислительной физики в теории твердого тела. Электронные состояния в неидеальных кристаллах. Киев : Наук. Думка, 1986. 296 с.

20. Local electron structure and magnetization in β – $Fe_{86}Mn_{13}C$ / L. I. Kveglis [et al.] // Superlattices and Microstructures. 2009. Vol. 46, No 1–2. P. 114–120.

21. Кулькова С. Е., Валуйский Д. В., Смолин И. Ю. Изменения электронной структуры при B2-B19′ мартенситном превращении в никелиде титана // Физика твердого тела. 2001. Т. 43, № 4. С. 706–713.